Shaft Capacity Assessment of Recharge Impulse Technology Piles

Wafi Bouassida[1], Essaieb Hamdi[1], Mounir Bouassida[1], and Yuri Kharine[2]
[1]*Université de Tunis El Manar/ Ecole Nationale d'Ingénieurs de Tunis. Laboratoire de Recherche Ingénierie Géotechnique, LRI4ES03 BP 37 Le Belvédère, 1002 Tunis. Tunisia.*
[2]*Rita Fondations. Tunis, Tunisia*
E-mail: mounir.bouassida@enit.utm.tn

ABSTRACT: This paper discusses the performance of Recharge Impulse Technology (RIT) in increasing the shaft capacity of deep foundation systems regarding classical set-up processes. Based on the major contributors behind such performances: the shape effect and the electrical discharge installation, a case study is analyzed in view of highlighting that the coupling of these two components leads to a reasonable estimation of RIT shaft capacity with reference to in situ loading tests. A related design chart estimating the contribution of the shape effect in the increase of the shaft capacity had been drawn and a mean power law was proposed through a parametric study on the adhesion factor.

KEYWORDS: Load test, Pile, Recharge impulse technology, Shaft capacity.

1. INTRODUCTION

The idea of improving the shaft capacity (with reference to bored piles) by means of a vibration source (i.e. driving) dates since more than thirty years in pile technology. Recent techniques in this context had coupled the classical driving process with new procedures to enhance this performance. As an example, inventors of full displacement piles technique as reported by Pucker and Grabe (2012) had added the rotation during the installation of their columns with a little enlargement of the pile section. This induced a remarkable improvement of relative densities of sandy layers crossed by such a setup process and so on the shaft capacity.

A more recent technique than full displacement piles, named concrete pipe pile (PCC), had also gained its use in China, peculiarly in highways and railways embankments. This is majorly due to the use of expansive concrete after the driving, which further ameliorates the shaft capacity compared to classically driven columns. For deeper information in this context, the framework of Zhou et al (2017) rigorously details how the expansion of concrete could increase the shaft capacity by more than 50% compared to the installation of classical PCC. However, in an urban construction context, driving piles in sands or in clays could cause harmful effects to nearby structures if they exist. This is naturally due to the frequencies of vibrations, developed during driving, that could approach one of the natural frequencies of the nearby structures and, hence, a resonance phenomenon is to be triggered. Indeed, serious harmful accidents had occurred during the installation of driving piles. As an example, during the construction project of the Damietta branch bridge (Egypt) the driving installation had yielded to the pier crack of the delta dam (Abdel-Rahman, 2001). Lewis and Davie (1993), Marr (2001) and Abdel-Rahman (2001) provided detailed explanations of the risk by pile driving to nearby structures.

In this context, the geniuses of recharge impulse technology came to encounter these issues. More precisely, Recharge Impulse Technology (RIT) proposes the improvement of the shaft capacity of a given deep foundation system without harming nearby constructions. This is clearly due to the extremely high frequency range of its vibration source (shock waves by electrical discharges) that is far away from the natural frequencies interval of any building structure. Thus, when exerting the electrical discharge, nearby structures "filtrate" the signal coming from RIT and remain stable. Consequently, RIT represents as a fashionable technique, which is suitable for practice in urban constructions and modern buildings without risks of harming historical monuments and nearby constructions.

This paper studies the shaft capacity performance of such a pile technology with reference to its two major components: the shape effect and the electrical discharge effects. A clarified description of the installation process of RIT piles with referenced projects are available in Bouassida et al (2016).

In this work, the performances of RIT piles are detailed. Then, the investigation of a case study high aims the highlighting of beneficial aspects of RIT piles compared to classical bored piles. A correlation between the shaft capacity ratio and the adhesion factor is proposed.

2. PERFORMANCES OF RIT PILES

2.1 Electrical Discharge

When exerting a lateral shock wave in a soil layer by means of an electrical discharge, the relative density increases and, accordingly, the shear strength is improved as well (RITA 2005). In this context, RIT experience in saturated silt sands had shown that horizontal compaction induced by the electrical discharge yields to an increase of relative density, friction angle, and cohesion of surrounding (RITA 2005). Equally, Alexandrovitch (2006) had studied the effects of electrical RIT discharges on the relative density of sand samples from which a remarkable decrease in the void ratio (hence an increase in the relative density) was observed after such a treatment. Thus, the frictional contact between a RIT pile and a set of surrounding soil layers is clearly higher than that of a bored circular pile and the same horizons due to the electrical discharge effect (Figure 1).

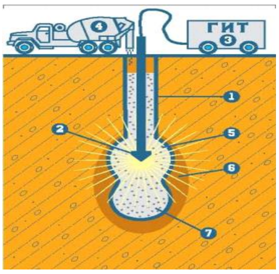

Figure 1 Set-up process of RIT piles (RITA, 2005)

This naturally yields to an increase in shaft bearing capacity of RIT piles regarding bored piles. Compared to driven piles, Recharge Impulse Technology differs in two main issues. The first one is the soil compaction, done at constant volume for RIT piles, contrary to the driven installation that allows heave during the set-up process (Poulos and Davis 1980) and, therefore, the volume variation. The second issue is related to the type of compaction itself. Indeed, the dynamic loading force transmitted to surrounding soil layers is different. For driven piles, one can model the vibration transmitted to surrounding layers as a classical wave producing the pore pressure dissipation. Conversely, the electrical discharge, which can be modeled as an impulse, does not produce pore pressure dissipation as the duration of such a blasting load is extremely short (An et al 2011). Hence, although driven piles and RIT foundations yield to a densification of surrounding soil layers and, therefore, an improvement of shaft bearing capacity, the two set-up processes differ and do not produce the same effect. Nowadays, since the pile codes do not propose recommendations for modeling the effect of blasting loads on surrounding soil layers and therefore on pile bearing capacities, it is obvious to find a gap between in situ load capacities of RIT piles and computed ones according to such standards. Hence, an accurate modeling of the electrical discharge installation brings us closer to RIT piles behavior and, consequently, allows a more realistic estimation of RIT load capacities.

2.2 Shape effect

As the final shape of an installed RIT pile is not cylindrical but rather constituted by bulbs, the frictional mechanism developed around the loaded pile differs from that developed around a cylindrical loaded pile. Indeed, for a cylindrical pile subjected to a vertical force, the maximum mobilized frictional contact along the soil-pile interface is:

$$\tau = C_a + K_s . \sigma \tan(\delta) \quad (1)$$

τ = the ultimate shear stress,

σ = the total or effective normal stress (depending on drained or undrained condition case)

C_a = soil-pile adhesion that is lower than soil cohesion, (Poulos and Davis, 1980).

K_s = Coefficient of earth pressure determined as:

$$K_s = (1 - \sin(\varphi))\sqrt{OCR}$$

δ = Friction angle between pile and soil. It varies between 1/3 φ (Pucker and Grabe, 2012) where φ is the soil friction angle.

OCR = over consolidation ratio.

Clearly, the shear stress along the contact surface between the pile and the soil is characterized by an interface friction angle lower than φ and a soil-pile adhesion lower than the cohesion of surrounding soil. For the case of RIT piles, and without considering the installation effect (electrical discharge compaction) improving both the friction angle and cohesion of the surrounding medium, the confined zones between the bulbs of a RIT pile, do not develop a shear stress along the pile-soil interface during the pile loading. Indeed, the frictional mechanism generated during the pile loading will mainly be developed at the contact boundaries (CB) of these zones, with the surrounding soil and not with the soil-pile interface (Figure 2).

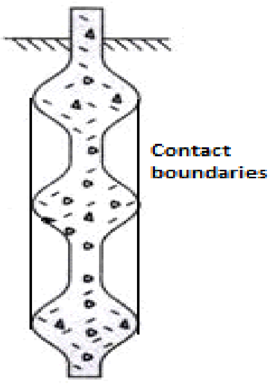

Figure 2 Frictional mechanism developed for loaded RIT pile

Such a mechanism produces therefore a vertical shear plan governed at failure by the friction angle and the cohesion of the surrounding soil (being aware that the thickness of bulb summits are much lower than the length of contact boundaries). Hence, the mobilized shear stress, in the failure phase of vertically loaded pile writes:

$$\tau = C + K_s . \sigma \tan(\varphi) \quad (2)$$

Consequently, according to equations (1) and (2) the frictional contact between a RIT pile and a set of surrounding soils is greater than that of a cylindrical pile and the same soil layers due to the curvy shape of RIT piles. Such a frictional mechanism, developed when loading a RIT pile, is similar to the frictional contact of under reamed piles, composed by bulbs, and widely used in India (Poulos and Davis 1980). Indeed, pull-out in situ tests carried by Mohan in 1977 (cited by Poulos and Davis, 1980) had confirmed that the frictional mechanism related to a given pile composed by bulbs, is developed during the loading phase, along the cylinder encountering the bulbs. Consequently, the shear stress distribution will be governed by friction angles and cohesions of surrounding soil layers (C, φ) and not the shear parameters characterizing the frictional contact between cylindrical piles and the surrounding soil layers (C_a, φ_a).

To confirm the consistency of such a mechanism for RIT piles, a pull-out test was conducted on a RIT pile of 6 meters length with an initial drilling diameter of 0.32 meter. Figure 3 presents the extracted pile with portions of soils confined between the bulbs. Further, the measurement of pile perimeter indicated that the diameter of the uplifted pile equals 0.4 meter. This confirms the 25% increase in diameter brought by the electrical discharge as stated by Bouassida et al (2016). Hence, and similarly to the electrical discharge, it should be stated that the curvy shape of a RIT pile is a major parameter that increases its shaft bearing capacity compared to cylindrical piles. Investigation of the contribution of these two parameters on the performance of RIT piles through analysis of a case study is presented, hereafter.

Figure 3 Coring concrete samples from the extracted RIT pile (L = 6 m, D = 0.4 m, Essalema suburb, Tunis City)

3. CASE STUDY

3.1 Site conditions

Investigated site is located at Essalema City (suburb of Tunis City) with a soil profile characterized by superposed silt and clayey layers having weak pressuremeter characteristics up to 60 meters depth. It is noted, between 25 and 29 m depth, the presence of a relatively stiff layer with a significant increase in pressuremeter modulus. Thus, a deep foundation solution was decided, consisting in a raft resting on a floating RIT piles group embedded one-meter depth within the stiff layer. Table 1 and Figure 4 present the results of the corresponding geotechnical campaign.

Table 1 Cohesions and friction angles of crossed layers

Layer	Thickness (m)	Cohesion (kPa)	Friction angle (°)
Brown Clayey sand	5	0	25
Silt Tunis soft clay	10	20	10
Dark Silt Clay	12	30	10

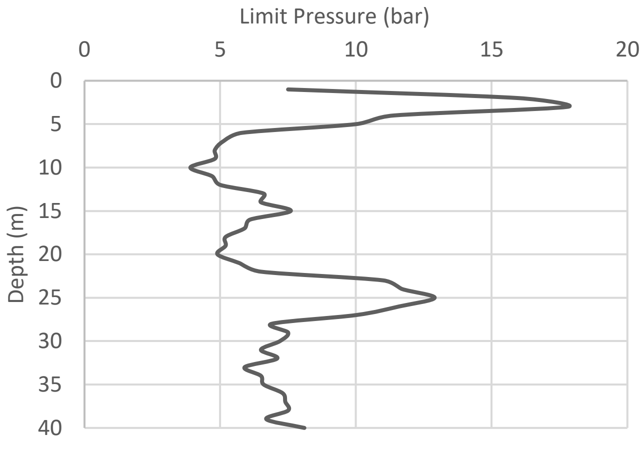

Figure 4. Variation of net limit pressure versus depth; 1 bar = 100kPa

3.2 Bearing capacity predictions

Bearing capacity of a single pile of diameter D=0.4 m and length L=20.5 m is predicted by two methods in the following.

1) *Predictions using pressuremeter test data (PMT):* According to PMT results plotted in Figure 4, the load capacities of a single cylindrical pile in the service state (factor of safety = 2), are presented in Table 2.

Table 2 Service load capacity of a single pile (D=0.4 m, L=20.5 m) according to the PMT

Pile capacity	Bearing Capacity (kN)
Shaft component	453
Tip component	57
Total Load Capacity	510

2) *Predictions according to C-φ method:* Using values of undrained cohesions and friction angles (obtained from undrained direct shear tests) presented in Table 1, the determination of ultimate bearing capacity of the same single pile according to C-φ method was evaluated. Adhesion factors had been chosen to be equal to 0.5 for all the layers in contact with the designed pile. This suitably agrees with the previous studies and recommendations of Poulos and Davis (1980) for normally consolidated and slightly over-consolidated clays. Moreover 66% of undrained friction angles had been employed to estimate the shaft and tip components (NAFVAC DM 1982). Table 3 presents the obtained results.

Table 3 Load capacity of a single pile (D=0.4 m, L=20.5m) according to C-φ method

Pile capacity	Bearing Capacity (kN)
Shaft component	430
Tip component	42
Total Load Capacity	472

3.3 Loading test

Figures 5 illustrates the results of the load-settlement curve of an axially loaded RIT pile (D=0.4 m, L=20.5 m). According to Figure 5, a vertical force of 1000kN yields to 4.4 mm of settlement.

Hence, this load is convenient for the service design since it corresponds to an admissible settlement. However, according to both PMT and C-φ methods, the admissible load capacities should not exceed 510kN. Consequently, one can clearly remark the underestimated load capacity of a RIT pile with reference to loading test results. Meaning that the behavior of a RIT pile, especially the frictional one, is quite different from the one of cylindrical pile. Hence, a correct estimation of such behavior, by using the standard of available codes, is difficult. In order to confirm this statement, a numerical model was built up to simulate the loading test of a cylindrical pile having the same equivalent characteristics (outer diameter and length) of the described RIT pile (D=0.4 m, L=20.5 m) and in contact with the same surrounding layers. This analysis is detailed in the following.

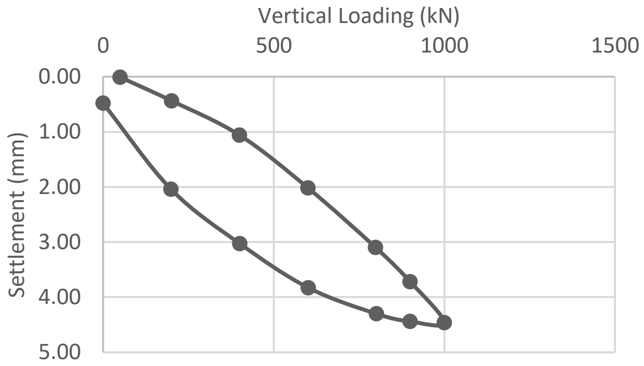

Figure 5 Load-settlement curve from a static load test executed on a RIT pile (D=0.4 m, L=20.5 m)

3. NUMERICAL MODELING OF STATIC LOAD TEST

In axisymmetric condition, a conventional cylindrical pile having the equivalent dimensions of the studied RIT pile (D=0.4 m, L=20.5 m) and in contact with the same layers described in section 1 had been subjected to a compressive loading test. Figure 6 shows the load-displacement curves corresponding respectively to the static loading test of a RIT pile, the elastic method (Poulos and Davis, 1980), and the numerical loading test.

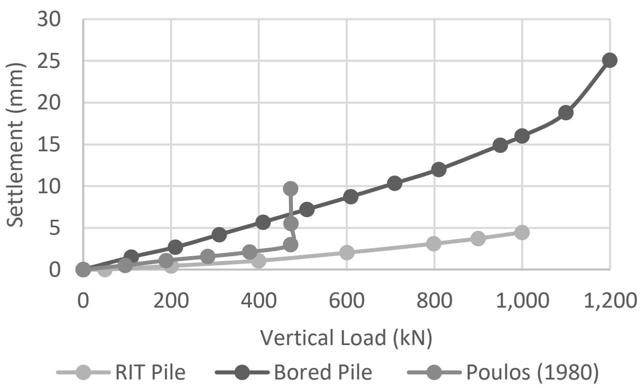

Figure 6 Comparison between the behavior of RIT pile (RP) and a cylindrical bored pile (CP)

According to the plot of the bored pile (obtained numerically), the load capacity should not overpass 400 kN to guarantee an admissible settlement. In the same context, the elastic load settlement curve drawn using the Poulos method indicates a full-mobilized shear resistance along the pile interface beyond 470 kN and a maximum settlement of 5.5 millimeters. Taking account of the pressuremeter load capacity (510 kN), the results lead to conclude that the design load is limited to 470 kN. Conversely, the installed RIT pile seems to offer a higher frictional performance as the slope of its load-settlement curve does not present a drastic decrease in the range of vertical load from 0 to 1000 kN. Equally, such a range offers a set of largely admissible settlements with a maximum value of 4.4 millimeters. Hence, the design load of a RIT pile in this case equals at least 2 times the load capacity of a bored floating pile having an equivalent geometry. As mentioned in the two first sections, the major parameters behind such a performance are the electrical discharge and the shape effect. More precisely, these two components should be taken into account for estimating the load capacity of RIT piles. In the following, the contribution of these two parameters in the enhancement of RIT load capacities compared to bored cylindrical piles is quantified.

3.1 Contribution of shape effect

According to Figure 2, estimating the shaft capacity of a RIT pile is equivalent to the estimation of the shear load developed around the cylindrical surface of the studied RIT pile. Following the c-φ method the ultimate shaft load capacity is:

$$Q_{su} = P\int_0^{L_1}(C + Ks.\sigma \tan(\varphi))dz + P\int_0^{L_2}(C_a + Ks.\sigma \tan(\varphi_a))dz \quad (3)$$

L_1 = Length between the bulbs summits in which there is a soil-to-soil shear.
L_2 = Length along which there is a soil-pile shear (L_2 equals the sum of vertical heights of the bulbs summits).
P = Perimeter of the pile having a circular cross section.

Considering that L_2 is much lower than L_1 ($L_2 << L_1$), the shaft load capacity reduces to:

$$Q_{su} = P\int_0^{L}(C + Ks.\sigma \tan(\varphi))dz \quad (4)$$

Integrating this relationship over the length of a RIT pile (L=20.5 m, D=0.4 m) embedded in the studied geotechnical strata yields to a shaft load capacity of 727 kN by adopting a factor of safety equals 2.

Further, the shaft capacity of a cylindrical pile is obtained by using the integral form of equation (3) between zero and L (i.e. along the length of the pile). For normally consolidated and slightly over-consolidated clays, the soil- pile adhesion factor C_a/C_u varies between 0.25 and 0.7 (Poulos and Davis 1980). Measurement of this parameter is missed for the studied project. Figure 7 presents the evolution of the shaft capacity of a bored cylindrical pile (embedded in the strata above described, D=0.4 m, L=20 m) as a function of the adhesion factor C_a/C_u for an interface friction angle φ_a varying between "1/3" and "2/3" of the surrounding layers friction angles.

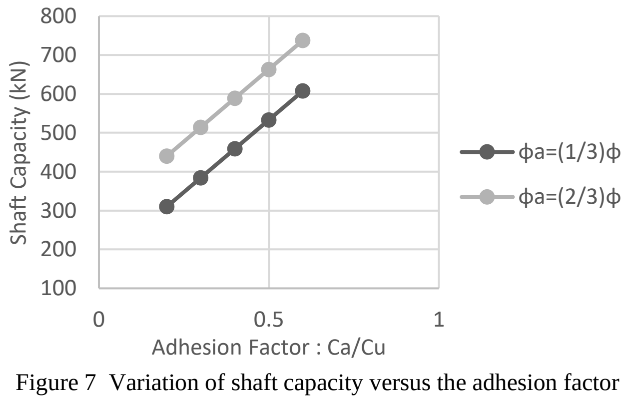

Figure 7 Variation of shaft capacity versus the adhesion factor C_a/C_u of a bored pile (L=20.5 m, D=0.4 m)

It is clear herein that the more adhesions are close to cohesions of surrounding layers, the more the shaft capacity increases as the contact between surrounding soil layers and the pile generates a greater shear resistance. Figure 8 highlights the contribution of the shape effect in the enhancement of the shaft load capacity for a RIT pile compared to a cylindrical pile. This figure shows the variation of the shaft capacity ratio which is defined by the shaft load capacity of a RIT pile divided by the shaft capacity of a bored cylindrical pile) as a function of the adhesion factor. Soil-pile friction angles are in between (1/3)φ and (2/3)φ.

According to Figure 8, it is remarkable that below an adhesion factor of 0.4, the shaft capacity ratio drastically increases. After the proposed average adhesion factor by Poulos and Davis (1980), for bored cylindrical piles in normally consolidated clays (equal to 0.5), one obtains a shaft capacity twice (an average value between the two curves) the shaft capacity of a circular pile having the same dimensions thanks to the soil-to-soil contact mechanism developed during the loading of a RIT pile. In this context, Salgado et al (2007) had conducted extensive parametric analysis on the adhesion factor and found that such a parameter varies between 0.38 and 0.73. This factor increases with the percentage of clay content. This finding is in agreement with both the envelope (0.25 - 0.7) and the average adhesion factor of 0.5, as proposed by Poulos and Davis (1980). For the studied case, the average variation of the shaft capacity ratio as a function of the adhesion factor is described by equation (5):

$$\frac{Qs(RITPile)}{Qs(BoredPile)} = 1.314\left(\frac{C_a}{C_u}\right)^{-0.549} \quad (5)$$

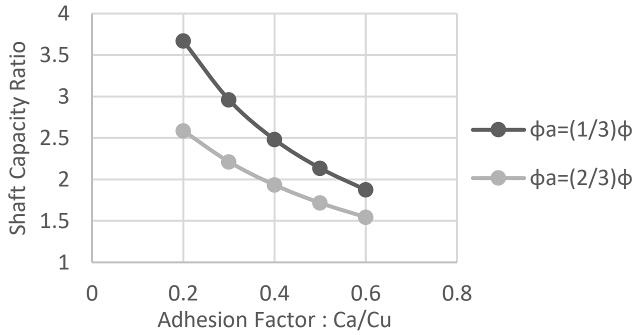

Figure 8 Envelope of the shaft capacity ratio as a function of the adhesion factor

3.2 Electrical discharge contribution

The contribution of the electrical discharge to the frictional performance of RIT piles was investigated in this project through a pressuremeter test carried nearby an executed RIT pile, located at the corner of the building under construction. Figure 9 presents the net limit pressure profile before and after the electrical discharge installation. From Figure 9, the improvement rate brought by the electrical discharge is clearly visible.

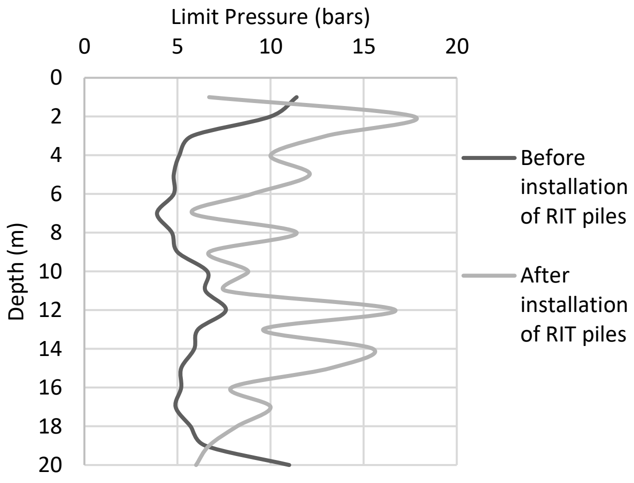

Figure 9 Net limit pressure profiles before and after the installation of RIT pile.

Indeed, the net limit pressure profile has shifted by a mean average value of more than 65% compared to the initial profile, i.e. before the installation of RIT pile. Hence, the shaft capacity will naturally increase. Table 4 presents the estimated load capacities of a cylindrical pile, of length 20.5 meters and a diameter of 0.4 m, after the pressuremeter data, for the service and ultimate states.

Table 4 Pile load capacities for ultimate and service states after the electrical discharge treatment

Load type	Shaft Load Capacity (kN)
Service load (FS=2)	936
Ultimate load (FS=1.4)	1310

Alternatively, it is possible to estimate the new undrained cohesions (after the electrical discharge) of the surrounding layers to the pile, from the improved net limit pressure profile, based on the correlations of Cassan (Kammoun et al, 2016):

$$0.3\ MPa < p_l < 1\ MPa \qquad C = \frac{p_l}{12} + 0.03 \qquad (6)$$

$$1\ MPa < p_l < 2.5\ MPa \qquad C = \frac{p_l}{35} + 0.085 \qquad (7)$$

Taking account of the shape effect contribution, presented in the previous section, Table 5 summarizes the enhanced undrained cohesions and the related shaft capacity of a RIT pile installed in the studied geotechnical strata.

Table 5 Shaft Load Capacity of a Single RIT Pile

Layer	Cohesion (kPa)
Brown Clayey sand	40.7
Silt Tunis soft Clay	36.6
Dark Silt Clay	60.2
Shaft Load Capacity	925 kN

The estimated shaft capacity (925 kN) by taking account of both, the electrical discharge and the shape effects, is fairly in agreement with the results of the static loading test. Indeed, the loading test results indicate that the design load should not overpass 1000 kN. Meaning that the use of the two presented parameters (shape effect and electrical discharge) yields to a consistent estimation of the shaft capacity (925 kN) regarding in situ test results (1000 kN). In terms of the ratio between the shaft capacity of a RIT pile and a bored cylindrical pile installed in the studied geotechnical strata, it is stated that the electrical discharge and the shape effects significantly increased the frictional performance of a RIT pile by a 2.45 factor compared to a cylindrical bored pile.

4. CONCLUSIONS

This paper focused on the contribution of shape effect in the increase of the shaft capacity of a RIT pile compared to that of classical bored cylindrical pile.

From a documented Tunisian case study, a proposed practical design chart allows the determination of the shape effect contribution in the increase of the shaft capacity of a RIT pile compared to a bored cylindrical pile. In addition, experimental investigation of the electrical discharge contribution, combined with the shape effect, showed that the coupling of these two components leads to a reasonable estimation of the shaft capacity of RIT pile.

Future works are in progress to develop a rigorous theoretical modelling of the cavity expansion due to the electrical discharge (taking account of the emergence of plastic shock waves in a porous medium) to be combined with the shape effect and hence to elaborate a complete framework for estimating the shaft capacity of RIT piles.

5. ACKNOWLEDGMENTS

Authors acknowledge Mr. Ahmed Amine Kammoun (Civil Engineer, Simpro consulting, Tunisia) for his contribution to the shape effect work. They equally express their gratitude to AfricSoil Company (Tunisia), which had carried the in-situ tests after RIT piles installation with a fair reasonable cost.

6. REFERENCES

Abdel-Rahman, S.M. (2012) “Vibration Associated with Pile Driving and its Effects on nearby Historical Structures”, Mechanical and Electrical Research Institute, National Water Research Center, Delta Dam, Egypt.

Alexandrovitch, B.A. (2006) “A Study on The Deformations of Malovlazhnogoed sand around RIT piles”, PhD Thesis, Moscow State University of Construction: 220 pages.

An, J., Tuan, C.Y., Cheesman, B.A, and Gazonas, G.A. (2011) “Simulation of Soil Behavior under Blast Loading”, International Journal of Geomechanics, Volume 11, No.4, pp323-334.

Bouassida. W, Hamdi, E., Bouassida. M, and Kharine. Y. (2016) “On the use of RITA pile technique in Tunisia”, Fourth International Conference on New developments in Soil Mechanics and Geotechnical Engineering, 2-4 June 2016, Near East University, Nicosia, North Cyprus.

Kammoun, A. A, Bouassida, W., and Bouassida, M. (2016) "Analyse de stabilité d'une excavation prévue pour la réalisation de l'OA 13 situé sur la ligne D du projet RFR Tunis", SIMPRO Tunisie. Rapport de validation, 22 pages.

Lewis, M.R., and Davie, J.R. (1993) "Vibrations due to pile driving", Third Int. Conf. on Case Histories in Geotech. Eng., St. Louis, Missouri, June 1-4, 1993, Paper No. 4.01.

Marr, W.A. (2001) “Dealing with Vibration and Noise from Pile Driving”, Pile Driving Contractors Association, Volume 2, No 1, 17-20.

Naval Facilities Engineering Command “NAVFAC” (1982) “Foundations & Earth Structures”, Design Manual 7.02. Virginia, USA; 279 pages.

Poulos, H.G., and Davis E.H. (1980) "Pile Foundations Analysis and Design", John Wiley and Sons. Vol. I: 397 pages.

Pucker, T., and Grabe, J. (2012) “Numerical Simulation of the Installation Process of Full Displacement Piles”, Computers and Geotechnics, Volume 45, pp93-106.

Recharge Impulse Technologies and Apparatus (RITA) (2005) “Building on the basement of knowledge”, RITA Press. Volume I: 58 pages. Moscow.

Salgado, R., Prezzi, M., and Seo, H. (2007) “Advanced Modeling Tools for the Analysis of Axially Loaded Piles”, Advances in Deep Foundations – Kikuchi, Otani, Kimura & Morikawa. Taylor & Francis Group. 438 pages.

Zhou, H., Hua. J., Ding, XM. and Chu, .J. (2017) “Theoretical Model for The Improved PCC Pile using Expansive Concrete”, Science China, Technological Sciences, Volume 60, No.5, pp772-791.